Journal Pre-proof

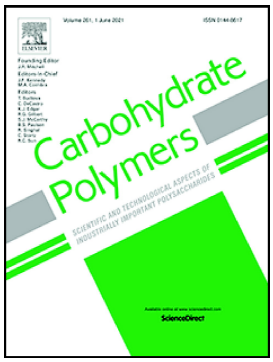

3D printed nanocellulose-based label for fruit freshness keeping and visual monitoring

Wei Zhou, Zhengguo Wu, Fengwei Xie, Shuwei Tang, Jiawei Fang, Xiaoying Wang

PII: S0144-8617(21)00932-2

DOI: https://doi.org/10.1016/j.carbpol.2021.118545

Reference: CARP 118545

To appear in: *Carbohydrate Polymers*

Received date: 21 April 2021

Revised date: 2 August 2021

Accepted date: 5 August 2021

Please cite this article as: W. Zhou, Z. Wu, F. Xie, et al., 3D printed nanocellulose-based label for fruit freshness keeping and visual monitoring, *Carbohydrate Polymers* (2021), https://doi.org/10.1016/j.carbpol.2021.118545

3D printed nanocellulose-based label for fruit freshness keeping and visual monitoring

Wei Zhou [a,1], Zhengguo Wu [a,1], Fengwei Xie [b], Shuwei Tang [a], Jiawei Fang [a], Xiaoying Wang [a]*

[a] State Key Laboratory of Pulp and Paper Engineering, South China University of Technology, 381 Wushan Road, Tianhe District, Guangzhou 510640, China

[b] International Institute for Nanocomposites Manufacturing (IINM), WMG, University of Warwick, Coventry CV4 7AL, UK

Email: xyw@scut.edu.cn

[1]These two authors contributed equally to this work.

Abstract

Food packaging systems with single function of freshness keeping or monitoring may not be able to meet all practical needs. Herein, cellulose nanofibers (CNF)-based labels with dual functions of fruit freshness keeping and visual monitoring were prepared by coaxial 3D printing. CNF-based ink with blueberry anthocyanin was used to create the shell of fibers, exhibiting high formability and print fidelity as well as sensitive visual pH responsiveness for freshness monitoring. Chitosan containing 1-methylcyclopropene (1-MCP) was loaded into the hollow microchannels of fibers, in which 1-MCP was trapped by the electrostatic effect of chitosan and CNF and exhibited sustained release behavior. The 3D printed labels prolonged shelf life of litchis for 6 days, meanwhile, they sensitively indicated the changes in freshness and the accuracy was confirmed by Headspace-Gas Chromatography-Ion Mobility

Spectrometry. The CNF-based integrated labels developed in this work provided a new idea for the development of food intelligent packaging.

Keywords: Three-dimensional printing, cellulose nanofibers, preservation, anthocyanin, 1-methylcyclopropene

1. Introduction

Intelligent packaging systems are developed to monitor the environmental conditions and quality of packaged food qualitatively or quantitatively in real time for meeting the increasing consumer demands in food safety (Choi, Lee, Lacroix, & Han, 2017; Ezati & Rhim, 2020; Fang, Zhao, Warner, & Johnson, 2017). The pH change of the environment inside the package is an important indication for informing food spoilage (Balbinot-Alfaro et al., 2019). Based on this mechanism, colorimetric pH indicators have been developed as a type of intelligent food packaging systems with the advantages of non-destructiveness, visualizability and low costs (Pourjavaher, Almasi, Meshkini, Pirsa, & Parandi, 2017; Prietto et al., 2017). PH-sensitive dyes are a significant part of visual colorimetric pH indicators which can be divided into synthetic and natural dyes (Pourjavaher et al., 2017). Dyes of natural origins are more suitable to be applied for food freshness monitoring due to their non-toxicity, biodegradability, and renewability (Balbinot-Alfaro et al., 2019; Liang, Sun, Cao, Li, & Wang, 2019; Pourjavaher et al., 2017). Among food-grade natural dyes, anthocyanins exhibit sensitive response in a wider pH range through color change. Therefore, anthocyanins can be used to realize real-time freshness monitoring and is an appropriate ingredient for developing visual colorimetric pH indicators (Choi et al., 2017; Guo et al., 2020; Roy & Rhim, 2020). However, most intelligent packaging

systems with anthocyanins do not possess the function of freshness keeping, but the latter is a big demand for intelligent food packaging, especially for fruits and vegetables (Liu et al., 2020). Hence, there is an increasing importance for developing intelligent packaging systems with both the functions of preservation and colorimetric pH indication.

1-Methylcyclopropene (1-MCP) is an ethylene receptor inhibitor with good freshness-keeping performance and no toxicity (Li et al., 2016; Zhu et al., 2020). Studies have shown that 1-MCP significantly delayed the ripening and softening of fruits and inhibited/reduced ethylene production, respiratory rate and the activation of genes related to aging and maturation of fruits (Du et al., 2020; Xu et al., 2019). Thus, 1-MCP can be used as a functional component in integrative intelligent packaging systems. However, the use of 1-MCP products in the form of tablet or powder is restricted due to their volatility and instability (Lin et al., 2018). Hence, it is essential to find an appropriate way to control the release of 1-MCP for long-lasting freshness keeping and can be conveniently used in practical applications. Moreover, the combined use of 1-MCP and anthocyanins is expected to realize the integration of freshness keeping and monitoring. Nonetheless, simple blending of anthocyanins and 1-MCP may interfere with each other causing inaccurate monitoring and insignificant effects. Core-shell structure is a suitable model since it has been proved to have the ability to protect sensitive payloads from the surrounding environment and controlling their release (Sperling, Reis, Pranke, & Wendorff, 2016; Wang et al., 2019). Furthermore, the hierarchical core-shell structure may reduce the interaction between components. Hence, the encapsulation of 1-MCP in core-shell fibers could be an appropriate solution.

The construction needs to be carried out under mild conditions due to the instability of anthocyanins and 1-MCP. From this point, coaxial 3D printing is an efficient and suitable way to fabricate core-shell fibers (Chen et al., 2020; Wang et al., 2020). Anthocyanins can be added to the shell for visual monitoring, and 1-MCP can be the core layer for its controlled release. 3D-built core-shell fiber is not only beneficial for 1-MCP embedding but also avoids the interaction between anthocyanin and 1-MCP, achieving the 3D printed label with a hierarchical structure and dual functions. In addition, it is vital to find an ideal matrix material, which can meet the rheological requirements of coaxial 3D printing, without compromising food safety. Cellulose nanofibers (CNF) would be a suitable candidate owing to the biocompatibility and shear-thinning behavior (Markstedt, Escalante, Toriz, & Gatenholm, 2017). Nevertheless, the viscoelasticity of pure CNF is not enough to support the printed structures. Alga polysaccharides such as sodium alginate (SA) and κ-carrageenan (KC) have been proven to effectively improve the viscoelasticity of the matrix (Mahendiran et al., 2021; Saha & Bhattacharya, 2010). Thus, they can be applied as auxiliary materials to tune the ink properties. Besides, the ionically crosslinkable sites of SA and KC could allow better fidelity to be achieved (Heggset et al., 2019; Kim, Lee, Jung, Oh, & Nam, 2019). Therefore, with the combination of CNF and alga polysaccharides such as SA and KC, a suitable printing ink is expected to be developed.

In this study, the two main demands of fruit preservation have been integrated in the 3D printed label to make up for the shortcomings of single-function packaging system. The feasibility and effectiveness of coaxial 3D printing as a new way to construct food intelligent packaging systems has been verified. Fruit freshness keeping and monitoring labels with high pH-sensitivity and effective shelf-life

extension capability have been successfully fabricated using coaxial 3D printing followed by ionic crosslinking (Fig. 1). 1-MCP was trapped due to the electrostatic effect of the chitosan core and the CNF shell, achieving its controlled release. The accuracy of the visual indication shown by the label can be confirmed by Headspace-Gas Chromatography-Ion Mobility Spectrometry (HS-GC-IMS). Employing coaxial 3D printing to construct integrated labels with both fruit freshness keeping and monitoring functions can provide an insight into the development of food intelligent packaging.

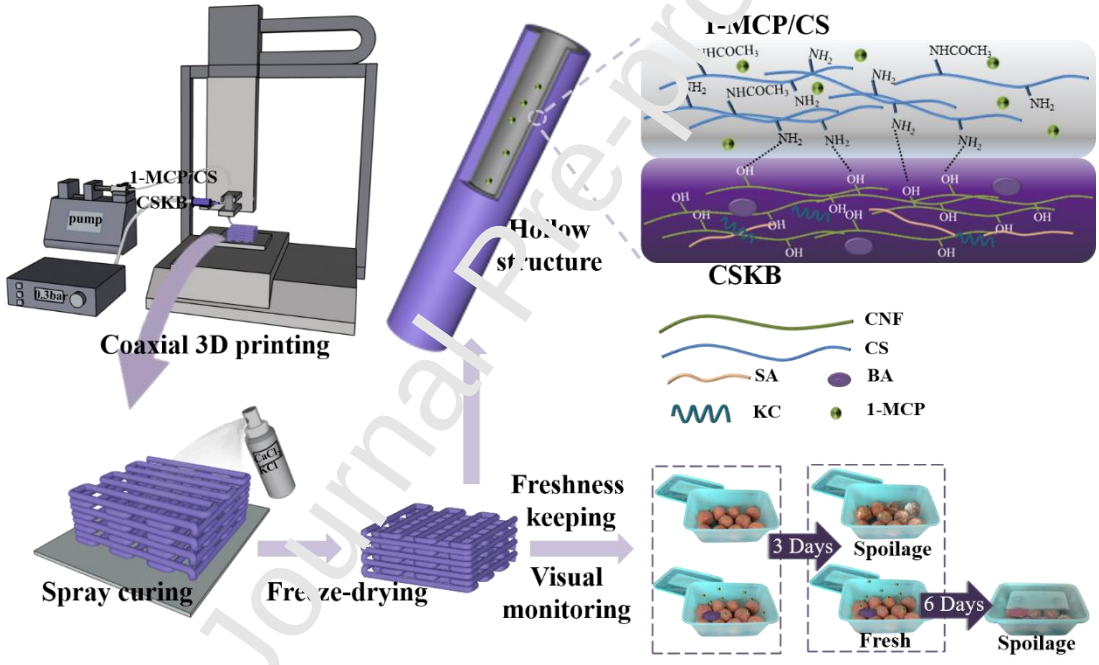

Fig. 1 Schematic diagram of the preparation process for 3D printed CNF-based labels and their application in food freshness keeping and monitoring (CNF: cellulose nanofibers, CS: chitosan, SA: sodium alginate, KC: k-carrageenan, BA: blueberry anthocyanin, 1-MCP: 1-methylcyclopropene).

2. Materials and methods

2.1 Materials

Cellulose nanofibers (CNF, hemicellulose content<10%) were purchased from Mujingling Biotechnology Co., Ltd. (Tianjin, China). The CNFs were processed from the bleached kraft pulp of coniferous wood (cellulose 78.2%, hemicellulose 20.1%, lignin 0.5%) in Tempo/NaBr/NaClO system. Sodium alginate (SA, from brown algae) and κ-carrageenan (KC) were purchased from Aladdin Industrial Co., Ltd. (Shanghai, China). L-(+)-lactic acid was purchased from Macklin Biochemical Co., Ltd. (Shanghai, China). 1-MCP was purchased from Xiqin Biotechnology Co., Ltd. (Xianyang, China). Blueberry anthocyanin (BA) (25%) was purchased from Shengqing Biotechnology Co., Ltd. (Xi'an, China). Chitosan (Cts) (M_w = 2.0 ×10^5 g/mol, 85% degree of deacetylation) was obtained from Haidebei Marine Bioengineering Co., Ltd. (Ji'nan China). All other chemicals were of analytical grade. The raw materials used in this study are all food contact approved.

2.2 Preparation of CNF-based inks and core solution

CNF-based inks: 0.1 g of SA (Calculated from Fig. S1 according to ASTM F2259-10 (2012), G/M ratio is 1.072) and 0.1 g of KC were added into 10 g of 5 wt% CNF with stirring to obtain an ink named CSK. 15 mg of BA (25%) was then mixed with CSK and the resulting ink is named CSKB. An ink named CSA was obtained by substituting KC in CSK for an equal weight of SA as a comparison group for the rheological study.

Core solution: Chitosan was dissolved in DI water containing 1% (v/v) L-(+)-lactic acid. Subsequently, 2.5 g of 1-MCP powder (3.3%) was dissolved in 10 mL of the chitosan solution (0.5% w/v). In this way, the core solution was prepared before immediate use.

2.3 Rheological tests of inks

The rheological properties of 5 wt% CNF and CNF-based inks were investigated by a rotation rheometer (ARES-G2, TA Instruments Co., Ltd., New Castle, USA) with a cone-plate geometry (diameter: 25 mm; angle: 0.0399 rad). The shear viscosity was measured with strain sweep from 0.01% to 100% with a fixed angular frequency of 6.2832 rad/s at 25 °C. Oscillation frequency measurements were conducted over an angular frequency range of 10^0–10^2 rad/s at 25 °C at a fixed strain of 0.5%. The flow sweep measurements were conducted over a shear rate range of 10^{-2}–10^2 at a frequency of 1 Hz at 25 °C. Samples were allowed to equilibrate at the designated testing temperature for 180 s prior to each measurement.

2.4 Preparation of labels

Coaxial 3D printing: A Dispensing Robot (YCD 7300N, Yida TEC Co., Ltd., Dongguan, China) was used to fabricate 3D printed labels, following specific steps:

Firstly, CSKB was introduced into a polyethylene injection cartridge, which was fixed onto the 3D printing device. The core solution (containing both chitosan and 1-MCP) was loaded into a 5 mL sterile injector and extruded by a syringe pump (LSP04-1A, Longer Precision Pump Co., Ltd., Baoding, China) at a speed of 3 mL/h. Square labels (25 × 25 × 5 mm^3) were printed layer-by-layer using a coaxial nozzle at a speed of 4 mm/s. The nozzle size was 17G/22G (424.31/1166.22 μm) and the extrusion pressure was about 0.3 bar. The printed labels were cured immediately by spraying them with a 2% (w/v) $CaCl_2$/KCl solution (2% (w/v) $CaCl_2$ and 2% (w/v) KCl in DI water mixture), followed by freeze-drying for 2 days. The printed label is named CSKB-MC.

A sample named CSKB-C was prepared by the same method mentioned above with CSKB as the 3D printing ink and the pure chitosan solution (without 1-MCP) as

the core solution. A sample named CSK-MC was prepared by the same method mentioned above with CSKB replaced by CSK. All abbreviations were in Table 1.

Table 1 Abbreviations of materials

Abbreviation	Description
CNF	cellulose nanofibers
CS	chitosan
SA	sodium alginate
KC	k-carrageenan
BA	blueberry anthocyanin
1-MCP	1-methylcyclopropene
CSA	cellulose nanofibers / sodium alginate
CSK	cellulose nanofibers / sodium alginate/ k-carrageenan
CSKB	cellulose nanofibers / sodium alginate/ k-carrageenan/ blueberry anthocyanin
CSK-MC	cellulose nanofibers / sodium alginate/ k-carrageenan-1-methylcyclopropene/ chitosan
CSKB-C	cellulose nanofibers / sodium alginate/ k-carrageenan/ blueberry anthocyanin -chitosan
CSKB-MC	cellulose nanofibers / sodium alginate/ k-carrageenan/ blueberry anthocyanin -1-methylcyclopropene/ chitosan

2.5 Characterization of labels

Scanning electron microscopy (SEM) images were obtained by a microscope (Merlin, Zeiss, Oberkochen, Germany). Fourier-transform infrared analysis was performed with an FT-IR spectrometer (FT-IR, VERTEX 70, Bruker, Germany) over a wavenumber range of 4000–400 cm^{-1}. X-ray diffractograms were obtained using a spectrometer (LEO1530VP, Zeiss, Oberkochen, Germany) with Cu Kα radiation over a 2θ range of 5–90°. The fibers of the samples obtained by coaxial 3D printing

(CSKB-C, CSK-MC, CSKB-MC) have been unfolded to expose their inner surface, and the corresponding XRD spectra were obtained by analysis of their inner surface.

2.6 pH-sensing evaluation

BA powder and the labels were immersed in different pH buffer solutions (2–12) respectively. The images of samples were collected under the same light source and 10 points on the images were randomly selected for analyzing the color of BA solutions (0.2 mg/mL) and the labels. The L^*, a^*, and b^* parameters of each point were extracted by Photoshop. The difference between colors is evaluated by the value of ΔE (Yong et al., 2019). ΔE was calculated from equation (1).

$$\Delta E = \sqrt{(L^* - L)^2 + (a^* - a)^2 + (b^* - b)^2}$$

In this equation, L (82.2), a (−2.9) and b (5.9) are the original color parameters of the background; L (54.3), a (15.7) and b (-10.4) are the original color parameters of the 3D printed labels.

2.7 Determination of 1-MCP release from the printed label

The release of 1-MCP from the printed label was monitored by Gas Chromatography (GC) (Agilent 7890A, Agilent Technologies, Inc., California, USA). Specifically, 1.0 g of 1-MCP powder was dissolved into 2 mL of DI water. The 1-MCP solution and the printed label were placed into 100 mL headspace-glass sampling vials, respectively, which were incubated at 40 °C for sampling. 20 mL of headspace was extracted for analysis. Injection and detector temperatures were set at 200 °C and 210 °C, respectively. The gas samples were separated with a KB-1701 capillary column equipped with a flame ionization detector. The column temperature was set at 110 °C. Nitrogen (99.999% purity) was used as the carrier gas.

2.8 Application of labels for litchi freshness keeping and monitoring during storage

Fresh litchis were purchased from Gaoshan Late-Ripe Litchi Garden in Kunming, China and transported to the lab via cold chain. The fruits selected for this study were uniform in weight (40 ± 5 g, 50 mm × 30 mm) and did not have visible mechanical damage or fungal infection. The litchis were randomly divided into four groups (20 litchis per group).

The control group received no treatment and the test groups were packaged with CSK-MC, CSKB-C and CSKB-MC, respectively. All groups were placed in a humidity chamber (LHS-50CL, Yiheng Scientific Instruments Co. Ltd., Shanghai, China) at 75% RH and 25 °C. Samples were evaluated by physicochemical analysis and Headspace-Gas Chromatography-Ion Mobility Spectrometry (HS-GC-IMS) after storage for 0, 1, 3, 5, 7, or 9 days.

Headspace-Gas Chromatography-Ion Mobility Spectrometry (HS-GC-IMS) Analysis: The analysis of litchi samples was performed by HS-GC-IMS (FlavourSpec, Gesellschaft für Analytische Sensorsysteme mbH, Dortmund, Germany) as described by Li et al. (Li et al., 2019) with slight modification. Specifically, 5.0 g of litchi pulp was placed into a 20 mL headspace-glass sampling vial. The samples were frozen with liquid nitrogen and stored at −80 °C. After incubation at 40 °C for 15 min, 200 μL of headspace was automatically injected into the injector under splitless injection mode with a syringe at 85 °C. Gas Chromatography was performed with an FS-SE-54-CB-1 (15 m, 0.53 mm ID) capillary column to separate volatile components and coupled to Ion Mobility Spectrometry at 45 °C. Nitrogen (99.999%) was used as the carrier gas under the following programmed flow: 2 mL/min for 2 min, then the rate increased from 2 mL/min to 100 mL/min during 18 min, and the flow stopped. The instrument was performed under ambient pressure. The analytes were separated at 60 °C in the column and then ionized in the ionization chamber at

45 °C. The drift gas (nitrogen gas) was set at 150 mL/min. In this experiment, the instrument was standardized with *n*-ketones whose retention index was linear. The retention index (RI) of volatile compounds was calculated using *n*-ketones C4-C9 (Sinopharm Chemical Reagent Beijing Co., Ltd., Beijing, China) as external references. Volatile compounds were identified by comparing RI and the drift time (the time it takes for ions to reach the collector through the drift tube, in milliseconds) with the standards in the library (Gesellschaft für Analytische Sensorsysteme mbH, Dortmund, Germany).

2.9. Statistical analysis

Duncan test and one-way analysis of variance were carried out using SPSS 24 software. Results were considered statistically different if $p < 0.05$.

3. Results and discussion

3.1 Rheology properties of CNF-based inks

The rheological properties of inks are key to 3D printing as they directly affects printability and fidelity (Sultan, Siqueira, Zimmermann, & Mathew, 2017). The rheological properties of CNF and CNF-based inks were investigated and the results are displayed in Fig. 2. As shown in Fig. 2a, both CNF and CNF-based inks possess significant shear thinning behavior with apparent viscosity reducing with increasing shear rate, which means the inks can be easily extruded (Shin, Kwak, Shin, & Hyun, 2019). Moreover, the addition of SA and KC significantly increased the zero shear viscosities to over 10^4 Pa·s. Interestingly, the curves of CNF-based inks with BA (CSKB) and without BA (CSK) almost overlapped, indicating that BA has almost no apparent effect on the rheological properties (Fig. 2a and b). Fig. 2b shows that the pure CNF exhibited high modules but low yield stress. For better formability and

fidelity, printing inks need to possess sufficient yield stress to support the printed shapes. After compounding CNF with sodium alginate and KC, the ink modules decreased slightly, accompanied by a significant increase in yield stress from 117.58 Pa to 255.24 Pa (Fig. 2b and S5a). In the case of equal additive mass, the CNF-based ink with both SA and KC (CSK) exhibited greater modulus and yield stress in comparison to that with the addition of only SA (CSA). Therefore, CSKB was chosen to be the CNF-based 3D printing ink for further investigation. As shown in S5b, the pure CNF sample with a uniform diameter of about 20 nm (Fig. S2 and S3) was in a gel state. The surface charge of CNF was about -75.58 mV (Fig. S4). CSA, CSK, and CSKB exhibited a more viscous and uniform gel state and the addition of BA did not affect this gel state.

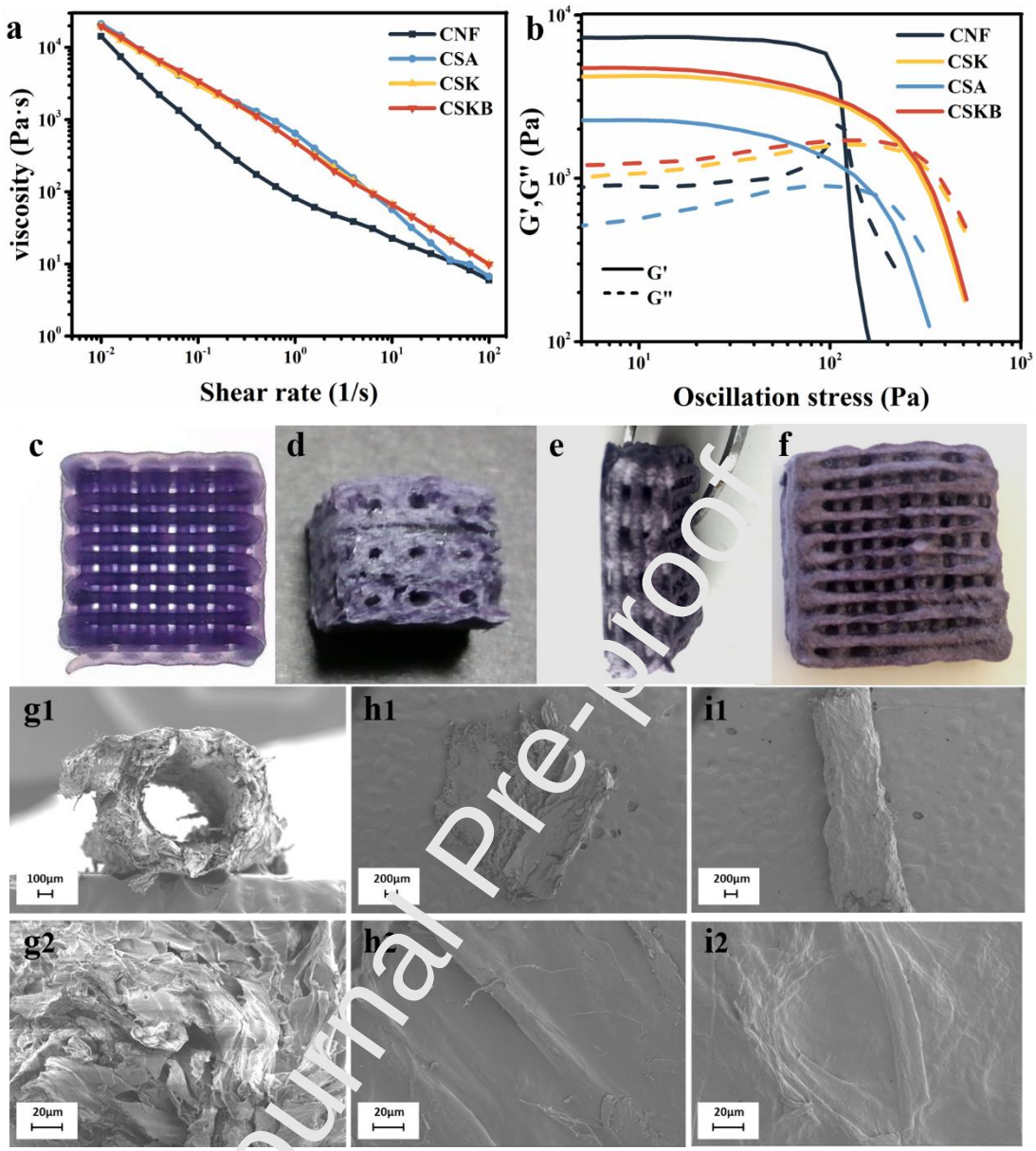

Fig. 2 (a) Steady-shear and (b) oscillatory rheological measurements. Morphology of the printed label CSKB-MC (c) in the wet state and (d-f) after freeze-drying. SEM images of (g1-g2) the section, (h1-h2) the inner surface, and (i1-i2) the outer surface of the printed label (CNF: cellulose nanofibers, CSA: CNF/SA, CSK: CNF/SA/KC, CSKB: CNF/SA/KC/BA, CSKB-MC: CNF/SA/KC/BA-1- MCP/Cts).

3.2 Morphology of 3D printed CNF-based labels

The manufacturing process of the 3D printed labels is displayed in Fig. 1. CSKB was the shell material and the 0.5 wt% chitosan dispersion containing 1-MCP was to

form the core. 1-MCP/chitosan was encapsulated within the fiber by a coaxial needle during printing. The extrudates were cured by spraying with a mixture solution of KCl and $CaCl_2$ followed by freeze-drying, and thus food freshness keeping and monitoring labels were obtained. As shown in Fig. 2c, the wet printed fibers possess uniform diameter and aligned arrangement, indicating the excellent formability and fidelity of the CSKB ink. After freeze-drying, the printed structures remained intact without collapse and deformation. The longitudinal section is shown in Fig. 2d, which indicates that internal channels with regular and clear structure were formed by water sublimation from the core solution. The morphology of the 3D printed label still maintained a complete grid shape and clear layering can be observed (Fig. 2e and f). SEM was employed to further investigate the structure of the printed core-shell fibers (Fig. 2g-i). Hollow micro-channels with a uniform diameter of about 700 μm were observed in Fig. 2g1. Its complete structure indicates that the CNF-based (CSKB) 3D printing ink possessed sufficient mechanical strength to support the hollow structure formed during freeze-drying. As shown in Fig. 2h1-h2 and i1-i2, the inner surface of the printed core-shell fiber was smoother than the outer surface, which was owing to the attachment of chitosan from the core solution. The moisture-mediated coating of chitosan during lyophilization can help the retention of 1-MCP in the hollow structure. More importantly, the possible electrostatic interaction between the inner chitosan and the outer CNF may trap 1-MCP on the inner fiber surface of the printed labels, leading to sustained release of 1-MCP for better freshness keeping.

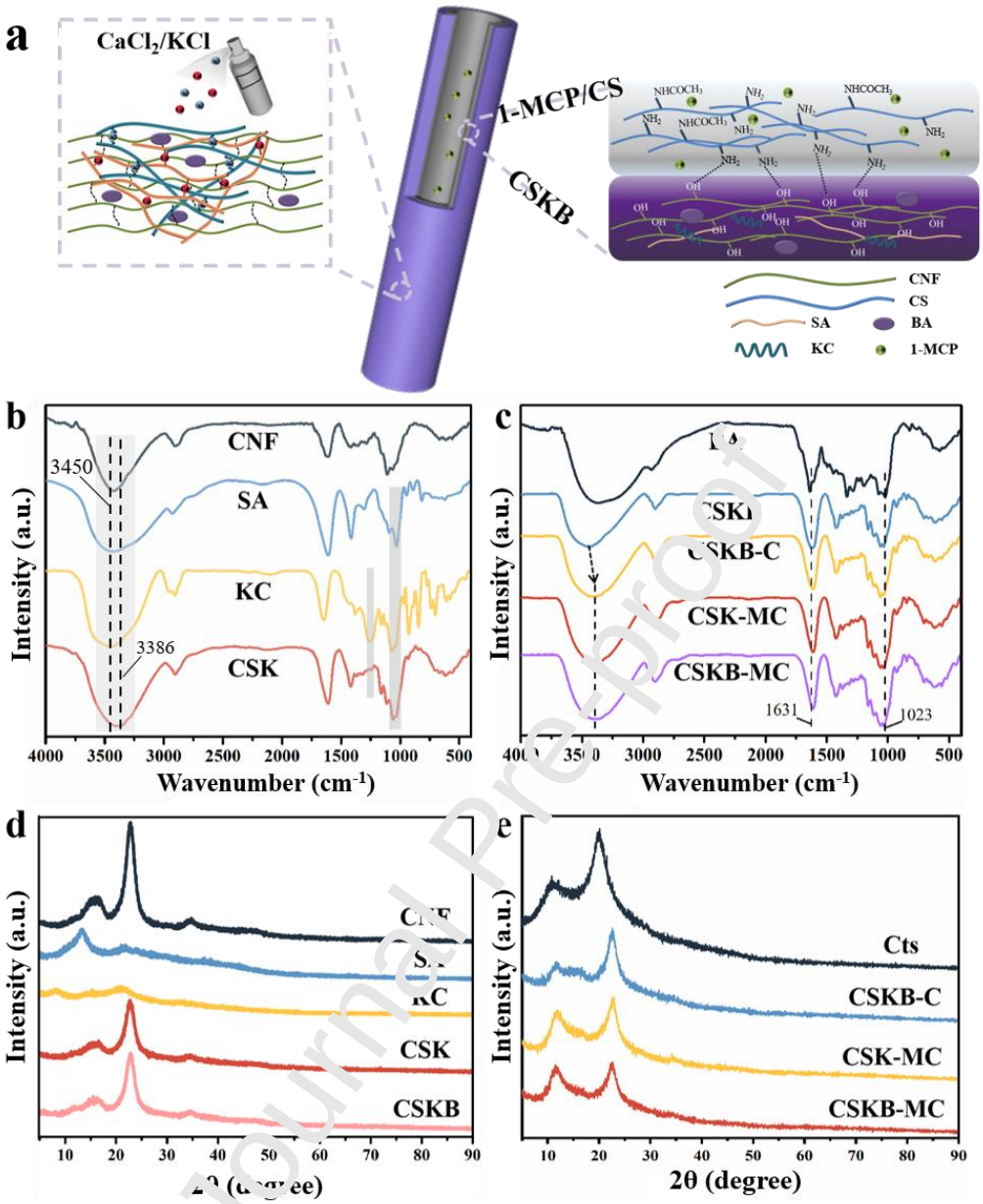

Fig. 3 (a) Schematic of the curing process and the core-shell interaction. (b, c) FT-IR spectra and (d, e) XRD patterns for the raw materials, CNF-based inks, and 3D printed labels (CNF: cellulose nanofibers, CS: chitosan, SA: sodium alginate, KC: k-carrageenan, BA: blueberry anthocyanin, CSK: CNF/SA/KC, CSKB: CNF/SA/KC/BA, CSKB-C: CNF/SA/KC/BA-Cts, CSK-MC: CNF/SA/KC-1-MCP/Cts, CSKB-MC: CNF/SA/KC/BA-1-MCP /Cts).

The FT-IR spectra were employed to investigate the interactions between components (Fig. 3b and c). As shown in Fig. 3b, the bands at ~3450 cm^{-1} in the

curves of CNF, SA and KC were related to the rich surface hydroxyl groups (Palaganas et al., 2017). The presence of peaks at around 2920 cm^{-1} was attributed to C–H stretching vibration (Palaganas et al., 2017). In the spectrum of SA, corresponding to the COO^- stretching, a characteristic peak was observed at 1417 cm^{-1}. As for the KC spectrum, the band at ~1260 cm^{-1} is attributed to the symmetric stretching vibration of O=S=O, indicating the presence of sulfate groups (Fan et al., 2011). The peaks at 930 cm^{-1} and 846 cm^{-1} represent the stretching vibration of C–O–C and C_4–O–S, respectively (Fan et al., 2011; Wang, Tang, Li, Zhang, & Kang, 2018). Therefore, the broad absorption band observed at 1027-1070 cm^{-1} in the spectrum of CSK was owing to the superposition of the COH stretching absorption band of SA at ~1030 cm^{-1} and the C–O stretching vibration of KC at ~1070 cm^{-1} (Abreu, Bianchini, Forte, & Kist, 2008; Fan et al., 2011). The characteristic bands of SA and KC presented in the spectra of CSK at ~1417 cm^{-1} and ~1260 cm^{-1} respectively. Moreover, in the spectrum for CSK, the band related to O-H stretching vibration blue-shifted to ~3386 cm^{-1} with increased band intensity compared with those for CNF, SA and KC (Fig. 3b), implying that strong hydrogen bonding was generated among components after mixing and gelation. Based on the above discussion, CNF, SA and KC were compounded to form the CSK ink successfully thanks to hydrogen bonding formed. As shown in Fig. 3c, the characteristic bands of BA were observed at 1023 cm^{-1} and 1631 cm^{-1}, which are ascribable to the O-C

stretching vibration of the anhydroglucose ring in flavonoid compounds and the C=C stretching vibration of the aromatic ring, respectively (Wu et al., 2020). These two characteristic bands were also visible in the spectra of the shell ink (CSKB) and the printed labels (CSKB-C, CSK-MC, CSKB-MC). In addition, there is no significant difference between the spectra for the printed label with both BA and 1-MCP (CSKB-MC) and for those with only BA (CSKB-C) or 1-MCP (CSK-MC), indicating that there is no obvious interaction between BA and 1-MCP. The FT-IR results show that CNF, SA, KC and BA were successfully combined to form a pH-responsive 3D printing ink (CSKB). Compared with the spectrum of CSKB, the bands of O-H stretching vibration blue-shifted in the spectra for all printed labels. Because cellulose nanofibers are negatively charged and chitosan is positively charged (Fig. S4), the blue shift is inferred to be related to the form of the electrostatic interaction between the chitosan in the core and the CNF in shell, as illustrated in Fig. 3a.

To further investigate the structure of the printed shell-core fibers, XRD analysis was performed and the results are displayed in Fig. 3d and e. The characteristic peaks of cellulose were presented in the spectra for both CNF and the CNF-based inks (CSK and CSKB), indicating that CNF was the main ingredients of the 3D printing inks. Moreover, there was no significant difference between the spectra for CSK and CSKB, implying that the addition of BA did not affect the crystallinity of the ink. As shown

in Fig. 3e, the spectra for CSKB-C, CSK-MC, and CSKB-MC all exhibited characteristic peaks of chitosan. Therefore, chitosan was proved to be attached to the inner surface of hollow shell-core fibers of the printed labels, which was conducive to the loading of 1-MCP. In Fig. 3e, with the addition of 1-MCP, the spectra for both CSK-MC and CSKB-MC showed an increase in peak intensity at 11.5°, indicating a change in the crystallinity of the material and the successful embedding of 1-MCP.

3.3 Characterization of the pH sensitivity of blueberry anthocyanin

The color variation of BA and the 3D printed labels in buffer solutions with different pH values was also measured and displayed in Fig. S6. Previous reports have proven that anthocyanins are pH-sensitive and their colors change with pH (Roy & Rhim, 2020). As shown in Fig. S6a, the chemical structure of anthocyanins changed with pH. In acidic conditions, BA exists as flavylium cations, showing red color. With an increasing pH value, the structure turns into quinoidal base, which appears in blue. With pH > 10, BA exists as the chalcone structure, and the solution of BA turns yellow (Yong et al., 2019). The UV-vis absorption spectra for BA under pH 2-12 are displayed in Fig. S6b and the corresponding colors of the solutions are shown in Fig. S6c. The shifting of the maximum absorption peak in the spectra was mainly caused by the structural transformation of BA at different pH values. The color parameters of BA in different buffers are summarized in Table S1, suggesting the high pH-sensitivity of BA. The color variation of the 3D printed labels (CSKB-MC) has also been characterized as shown in Fig. S6d and the color parameters were displayed in Table S2. ΔE was calculated by comparing with the origin dry label. $\Delta E > 3.5$ indicates that there was a clear difference in color which can be noticed (Halász &

Csóka, 2018). As shown in Fig. S6d and Table S2, ΔE values of the 3D printed label (CSKB-MC) at pH 2-12 are in the range of 12 to 40. Thus, the 3D printed labels can significantly indicate different pH values. Compared with similar packaging systems that use anthocyanins as pH indicators, the 3D printed labels have comparable or even more obvious visual indications of pH changes in terms of color parameters and exhibit sensitive pH responsiveness (Chi et al., 2020; Moradi, Tajik, Almasi, Forough, & Ezati, 2019). Thus, the 3D printed labels show great potential to monitor fruit freshness by providing real-time pH information about the inner package environment.

3.4 1-MCP release behavior of 3D printed CNF-based labels

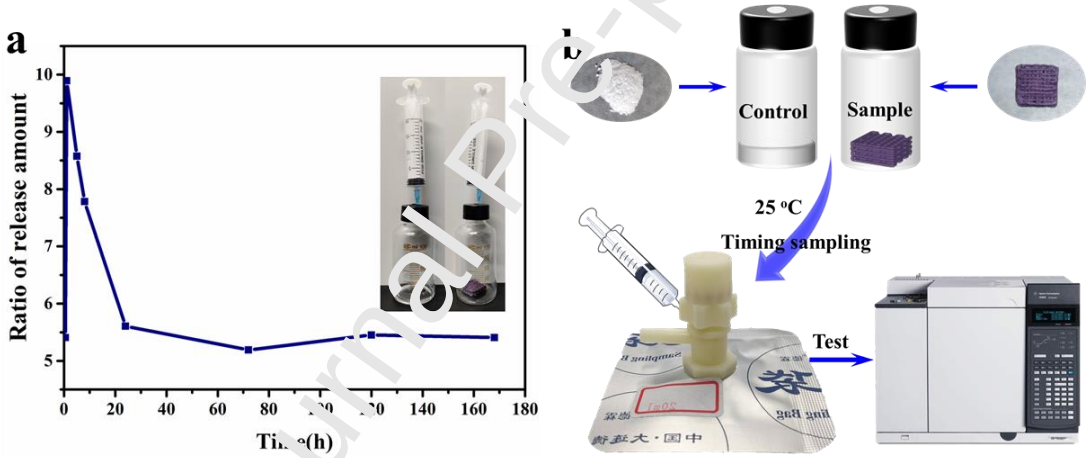

Fig. 4 (a) Release rate ratio of 1-MCP before and after embedding. (b) Schematic of the 1-MCP release experiment (1-MCP: 1-methylcyclopropene, Control: 1-MCP powder, Sample: (CSKB-MC) CNF/SA/KC/BA-1-MCP /Cts).

The differences in the 1-MCP release rate before and after being embedded in the 3D printed labels were analyzed by gas chromatography as shown in Fig. 4. Gas samples were taken out at a fixed time point. The released amount of the 1-MCP was obtained by integrating the release fluxes with time (Ariyanto & Yoshii, 2019). The release amount ratio of raw

1-MCP powder to the printed label (CSKB-MC) is shown in Fig. 4a. The ratio of release amount shows a trend of rising firstly and then falling. In the first 1 h, the release rate of raw 1-MCP powder increased sharply and it was significantly larger than that of the printed label. After 1 h, the release amount of raw 1-MCP powder was nearly 10 times that of CSKB-MC, and then the ratio decreased with time. Subsequently, the ratio of release amount stabilized after 24 h. This is because that the 3D printed label released 1-MCP continuously and smoothly while the release amount of the raw material remains almost stable after experiencing a peak. As shown in Fig. 4a, compared with the 3D printed label, the release rate of raw 1-MCP increased sharply in the early hours and dropped rapidly. Therefore, the 3D printed label had 1-MCP embedded effectively and could achieve long-term release for lasting freshness keeping effect.

3.5 Application of the 3D printed labels for litchis storage

In order to investigate the freshness keeping and monitoring performance of the printed label, a litchi freshness-keeping experiment was carried out (Fig. 5). In the control group, slight spoilage (red arrows) started to appear on day 3 and the situation deteriorated further in the following days. Severe spoilage occurred on day 5 as shown by white mildew spots all on the peel and peel depressions. The depressions intensified during the next few days, accompanied by the leakage of juice. The group with the use of the label without 1-MCP loaded (CSKB-C) showed the same spoilage process as the control group. In contrast, the group with CSK-MC and CSKB-MC showed a markedly slowing spoilage process with the first appearance of mildew

spots on the 9th day. This is most likely due to the slow and long-lasting release of 1-MCP embedded in CSK-MC and CSKB-MC. The slowly released 1-MCP bound to the ethylene receptors of litchis to delay the maturation and spoilage process of the fruit after harvest. In general, the printed labels effectively kept the freshness and prolonged the shelf life of litchis for 6 days at room temperature.

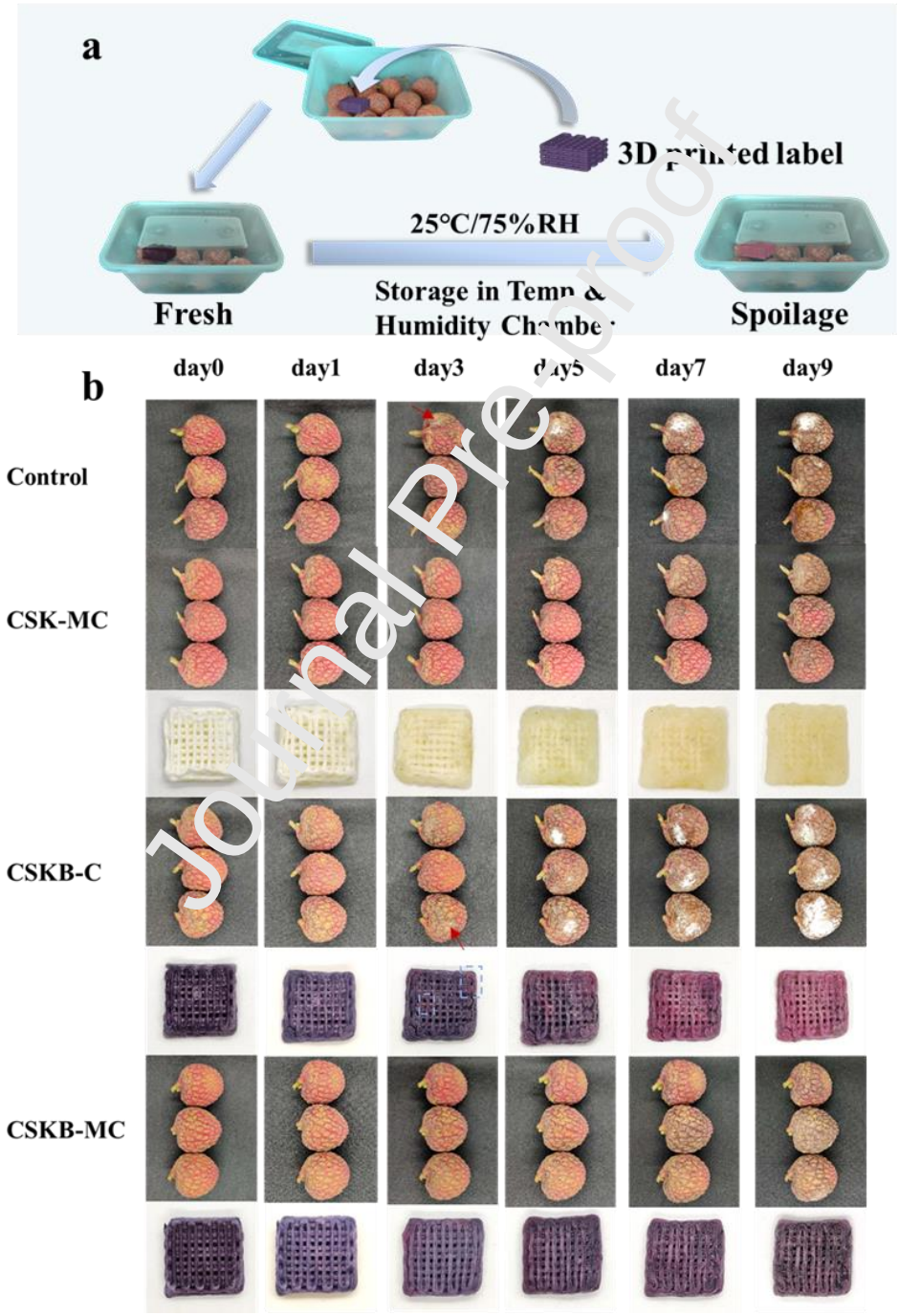

Fig. 5 (a) Schematic diagram of the freshness monitoring and preservation experiment of litchis. (b) Freshness keeping and monitoring performance of 3D printed labels during litchis storage (Control: no treatment, CSK-MC: CNF/SA/KC-1-MCP/Cts, CSKB-C: CNF/SA/KC/BA-Cts, CSKB-MC: CNF/SA/KC/BA-1-MCP /Cts).

As shown in Fig. 5, the color of the printed label without BA (CSK-MC) did not change although litchis have spoiled, while the color of the printed labels CSKB-C and CSKB-MC gradually changed from purple to pink during the storage of litchis. The color parameters of the labels during the storage of litchis were listed in Table S3. The color change of two adjacent sampling time points is evaluated by ΔE and all the values were above 3.5, indicating that the degree of color change can be detected by naked eyes (Halász & Csóka, 2018). Thus, during storage, a clear causal relationship between the freshness of litchis and the color change of the 3D printed labels have been observed. With a decrease in the freshness degree, the color of the label gradually changed from purple to pink. And the color changes of the labels can sensitively and visually indicate even slight spoilage of litchis which is hard to spot with naked eyes (red arrows).

Therefore, we have successfully constructed 3D printed CNF-based labels for fruit freshness keeping and monitoring purposes, which show great application potential for food intelligent packaging. The printed label does not need to strict contact with the corresponding fruit. It works by detecting pH changes of the environment inside the package. The mechanism of 1-MCP is to irreversibly bind with the ethylene receptors of fruits and vegetables, thereby delaying their ripening and corruption. So theoretically, the printed label has a general fresh-keeping effect on fruits and vegetables. Its applications on other fruits would be investigated in the future.

3.6 Differential analysis of volatile components in litchis at different storage periods

Many complicated changes occurred to the aromatic components of fruits during storage, such as vitamin degradation and phenol oxidation, leading to changes in fruit flavor (Yang et al., 2019). In order to evaluate the quality and flavor changes of litchis during storage as well as to further prove the accuracy of label indication, HS-GC-IMS was employed to analyze the differences of volatile organic compounds (VOCs) of litchi pulp in the control group and the CSKB-MC group at different storage periods. Fig. 6a is the 3D topographical visualization of the data, where the X-axis denotes the ion migration time for identification, the Y-axis represents the retention time of gas chromatography, and Z-axis represents the peak intensity. From the 3D topographic plot, it can be clearly observed that the released VOCs increased with a prolonged duration of storage.

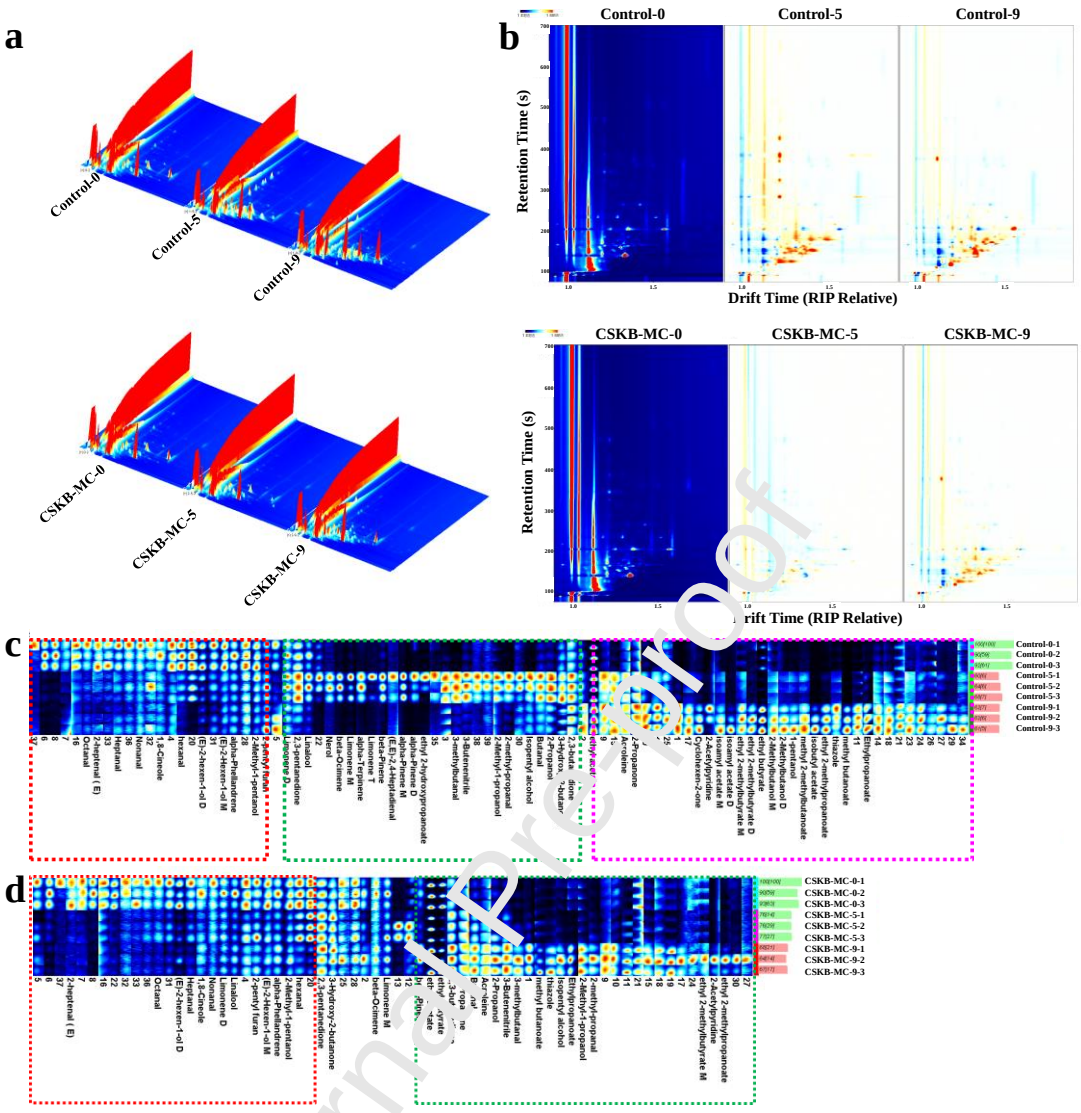

Fig. 6 (a) 3D- (b) 2D-topographic plots of litchis at different times. CSKB-MC-0, CSKB-MC-5, CSKB-MC-9 represent the litchis in the CSKB-MC group on day 0, 5 and 9. (c) Fingerprint of volatile compounds in litchis in the control group. (d) Fingerprint of volatile compounds in litchis in the CSKB-MC group (Control: no treatment, CSKB-MC: CNF/SA/KC/BA-1-MCP /Cts).

The top view of 3D topographic plots was displayed in Fig. 6b after deducting the background with the initial state as the reference. The VOCs with the same level as the reference were canceled out to show a white color, while blue represents the level of VOCs lower than that of the reference and red means the level of VOCs

higher than that of the reference. As shown in Fig. 6b, the change in the VOCs level in the CSKB-MC group was much smaller than that in the control group during the storage. The fingerprints of volatile compounds in the control group and the CSKB-MC group are exhibited in Fig. 6c and d, clearly revealing the compositional changes of released volatile compounds during litchis storage. The fresh litchi pulp on day 0 released small amounts of VOCs, which mainly consisted of aldehydes and alcohols (red-framed areas) and their contents decreased with the prolonged storage. After storage in the humidity chamber for 5 days, the content of VOCs framed in green (mainly terpenes) was relatively high in the control group. In contrast, the level of VOCs in the pulp of the CSKB-MC group was still low after storage for 5 days and no new volatile substances were produced. The difference of VOCs between control-5 and CSKB-MC-5 can be clearly observed in Fig. S7 and S9. More importantly, according to the PCA and proximal analyses (Fig. S11 and S12), the litchis pulp of CSKB-MC-5 was similar to that of Control-0 in VOCs level, indicating a significant difference in freshness between the control and the CSKB-MC group on day 5 and the excellent fresh-keeping effect of the 3D printed label. On day 9, there were more VOCs in control-9 than in CSKB-MC-9 (Fig. S8 and S10). According to the above results, the change in VOCs level for the CSKB-MC group was much smaller than that of the control group during the whole storage period, indicating that the presence of CSKB-MC slowed down the spoilage process of litchis. The results of HS-GC-IMS are consistent with the color information indicated on the labels, which proves the freshness monitoring sensitivity of CSKB-MC.

4. Conclusions

Coaxial 3D printing has hardly been employed in constructing food intelligent packaging. Constructing the core-shell fiber by coaxial 3D printing can integrate dual functions in one step and realize functional partitioning to avoid mutual interference. In this study, a CNF-based label with dual functions of fruit freshness keeping and visual monitoring was successfully fabricated by coaxial 3D printing with CNF/SA/KC/BA as the shell and CS/1-MCP as the core. The 3D printed label exhibited sensitive colorimetric pH response with BA in the shell layer. 1-MCP was trapped on the inner surface of hollow microchannels by electrostatic interaction between chitosan and cellulose, realizing controlled release and long-lasting fresh-keeping effects on litchis. The label prolonged the shelf life of litchis up to 6 days and sensitively indicated the changes in freshness during storage. The HS-GC-IMS results proved the high sensitivity and accuracy regarding the label freshness visual monitoring results. The dual-function integrated 3D printed label makes up for the shortcomings of single-function packaging system. This work provides a new idea for the development of food intelligent packaging.

Acknowledgements

This work was financially supported by the Guangdong Basic and Applied Basic Research Foundation (Nos. 2020B1515120038 and 2020A1515110004), the State Key Laboratory of Pulp and Paper Engineering (No. 2020ZR05), the Fundamental Research Funds for the Central Universities (Nos. 2020ZYGXZR066 and 2019PY13), the China Postdoctoral Science Foundation (No. 2020M682716), and Science and Technology Planning Project of Guangzhou City (No, 202102020007).

DATA AVAILABILITY STATEMENT

This manuscript comprises an original, unpublished material, which is not under consideration for publication elsewhere, and all authors have read and approved the text and consent to its publication. All experimental data are accurate and reliable.

COMPETING INTERESTS' STATEMENT

The authors declare no competing financial interests and any non-financial competing interests.

References

Abreu, F. O. M. S., Bianchini, C., Forte, M. M. C., & Kist, T. B. L. (2008). Influence of the composition and preparation method on the morphology and swelling behavior of alginate–chitosan hydrogels. *Carbohydrate Polymers*, *74(2)*, 283-289.

Ariyanto, H. D., & Yoshii, H. (2019). Effect of stepwise humidity change on the release rate constant of 1-methylcyclopropene (1-MCP) in a cyclodextrin inclusion complex powder. *Food Packaging and Shelf Life*, *21*, Article 100322.

Balbinot-Alfaro, E., Craveiro, D. V., Lima, K. O., Costa, H. L. G., Lopes, D. R., & Prentice, C. (2019). Intelligent Packaging with pH Indicator Potential. *Food Engineering Reviews*, *11(4)*, 235-244.

Chen, Y., Liu, Y., Ren, J., Yang, W., Zhang, E., Ma, K., Zhang, L., Jiang, J., & Sun, X. (2020). Conformable core-shell fiber tactile sensor by continuous tubular deposition modeling with water-based sacrificial coaxial writing. *Materials & Design*, *190*, Article 108567.

Chi, W., Cao, L., Sun, G., Meng, F., Zhang, C., Li, J., & Wang, L. (2020). Developing a highly pH-sensitive κ-carrageenan-based intelligent film incorporating grape skin powder via a cleaner process. *Journal of Cleaner Production*, *244*, Article 118862.

Choi, I., Lee, J. Y., Lacroix, M., & Han, J. (2017). Intelligent pH indicator film composed of agar/potato starch and anthocyanin extracts from purple sweet potato. *Food Chemistry*, *218*, 122-128.

Du, M., Jia, X., Li, J., Li, X., Jiang, J., Li, H., Zheng, Y., Liu, Z., Zhang, X., & Fan, J. (2020). Regulation effects of 1-MCP combined with flow microcirculation of sterilizing medium on peach shelf quality. *Scientia Horticulturae*, *260*, Article 108867.

Ezati, P., & Rhim, J.-W. (2020). pH-responsive chitosan-based film incorporated with alizarin for intelligent packaging applications. *Food Hydrocolloids*, *102*, Article 105629.

Fan, L., Wang, L., Gao, S., Wu, P., Li, M., Xie, W., Liu, S., & Wang, W. (2011). Synthesis, characterization and properties of carboxymethyl kappa carrageenan. *Carbohydrate Polymers*, *86*(3), 1167-1174.

Fang, Z., Zhao, Y., Warner, R. D., & Johnson, S. K. (2017). Active and intelligent packaging in meat industry. *Trends In Food Science & Technology*, *61*, 60-71.

Guo, M., Wang, H., Wang, Q., Chen, M., Li, L., Li, X., & Jiang, S. (2020). Intelligent double-layer fiber mats with high colorimetric response sensitivity for food freshness monitoring and preservation. *Food Hydrocolloids*, *101*, Article 105468.

Halász, K., & Csóka, L. (2018). Black chokeberry (*Aronia melanocarpa*) pomace extract immobilized in chitosan for colorimetric pH indicator film application. *Food Packaging and Shelf Life*, *16*, 185-193.

Heggset, E. B., Strand, B. L., Sundby, K. W., Simon, S., Chinga-Carrasco, G., & Syverud, K. (2019). Viscoelastic properties of nanocellulose based inks for 3D printing and mechanical properties of CNF/alginate biocomposite gels. *Cellulose*, *26(1)*, 581-595.

Kim, M. H., Lee, Y. W., Jung, W. K., Oh, J., & Nam, S. Y. (2019). Enhanced rheological behaviors of alginate hydrogels with carrageenan for extrusion-based bioprinting. *Journal Of the Mechanical Behavior Of Biomedical Materials*, *98*, 187-194.

Li, L., Lichter, A., Chalupowic, D., Gamrasni, D., Goldberg, T., Nerya, O., Ben-Arie, R., & Porat, R. (2016). Effects of the ethylene-action inhibitor 1-methylcyclopropene on postharvest quality of non-climacteric fruit crops. *Postharvest Biology And Technology*, *111*, 322-329.

Li, M., Yang, R., Zhang, H., Wang, S., Chen, D., & Lin, S. (2019). Development of a flavor fingerprint by HS-GC-IMS with PCA for volatile compounds of Tricholoma matsutake Singer. *Food Chemistry*, *290*, 32-39.

Liang, T., Sun, G., Cao, L., Li, J., & Wang, L. (2019). A pH and NH_3 sensing intelligent film based on *Artemisia sphaerocephala* Krasch. gum and red cabbage anthocyanins anchored by carboxymethyl cellulose sodium added as a host complex. *Food Hydrocolloids*, *87*, 858-868.

Lin, Y., Lin, Y., Lin, H., Lin, M., Li, H., Yuan, F., Chen, Y., & Xiao, J. (2018). Effects of paper containing 1-MCP postharvest treatment on the disassembly of cell wall polysaccharides and softening in Younai plum fruit during storage. *Food Chemistry*, *264*, 1-8.

Liu, X., Chen, K., Wang, J., Wang, Y., Tang, Y., Gao, X., Zhu, L., Li, X., & Li, J. (2020). An on-package colorimetric sensing label based on a sol-gel matrix for fish freshness monitoring. *Food Chemistry*, *307*, Article 125580.

Mahendiran, B., Muthusamy, S., Sampath, S., Jaisankar, S. N., Popat, K. C., Selvakumar, R., & Krishnakumar, G. S. (2021). Recent trends in natural polysaccharide based bioinks for multiscale 3D printing in tissue regeneration: A review. *International journal of biological macromolecules*, *183*, 564-588.

Markstedt, K., Escalante, A., Toriz, G., & Gatenholm, P. (2017). Biomimetic inks based on cellulose nanofibrils and cross-linkable xylans for 3D printing. *ACS Appl Mater Interfaces*, *9(46)*, 40878-40886.

Moradi, M., Tajik, H., Almasi, H., Forough, M., & Ezati, P. (2019). A novel pH-sensing indicator based on bacterial cellulose nanofibers and black carrot anthocyanins for monitoring fish freshness. *Carbohydrate Polymers*, *222*, Article 115030.

Palaganas, N. B., Mangadlao, J. D., de Leon, A. C. C., Palaganas, J. O., Pangilinan, K. D., Lee, Y. J., & Advincula, R. C. (2017). 3D printing of photocurable cellulose nanocrystal composite for fabrication of complex architectures via stereolithography. *ACS Appl Mater Interfaces*, *9(39)*, 34314-34324.

Pourjavaher, S., Almasi, H., Meshkini, S., Pirsa, S., & Parandi, E. (2017). Development of a colorimetric pH indicator based on bacterial cellulose nanofibers and red cabbage (*Brassica oleraceae*) extract. *Carbohydrate Polymers, 156*, 193-201.

Prietto, L., Mirapalhete, T. C., Pinto, V. Z., Hoffmann, J. F., Vanier, N. L., Lim, L.-T., Dias, A. R. G., & Zavareze, E. d. R. (2017). pH-sensitive films containing anthocyanins extracted from black bean seed coat and red cabbage. *Lwt-Food Science And Technology, 80*, 492-500.

Roy, S., & Rhim, J. W. (2020). Anthocyanin food colorant and its application in pH-responsive color change indicator films. *Crit Rev Food Sci Nutr*, 1-29.

Saha, D., & Bhattacharya, S. (2010). Hydrocolloids as thickening and gelling agents in food: a critical review. *J Food Sci Technol, 47*(6), 587-597.

Shin, S., Kwak, H., Shin, D., & Hyun, J. (2019). Solid matrix-assisted printing for three-dimensional structuring of a viscoelastic medium surface. *Nature Communications, 10*(1), Article 4650.

Sperling, L. E., Reis, K. P., Pranke, P., & Wendorff, J. H. (2016). Advantages and challenges offered by biofunctional core-shell fiber systems for tissue engineering and drug delivery. *Drug Discov Today, 21*(8), 1243-1256.

Sultan, S., Siqueira, G., Zimmermann, T., & Mathew, A. P. (2017). 3D printing of nano-cellulosic biomaterials for medical applications. *Current Opinion in Biomedical Engineering, 2*, 29-34.

Wang, N., Teng, H., Li, L., Zhang, J., & Kang, P. (2018). Synthesis of phosphated k-carrageenan and its application for flame-retardant waterborne epoxy. *Polymers (Basel), 10*(11), Article 1268.

Wang, Y., Jiang, Y., Zhang, Y., Wen, S., Wang, Y., & Zhang, H. (2019). Dual functional electrospun core-shell nanofibers for anti-infective guided bone regeneration membranes. *Materials Science & Engineering C-Materials for Biological Applications, 98*, 134-139.

Wang, Z., Ren, J., Liu, R., Sun, Z., Huang, D., Xu, W., Jiang, J., Ma, K., & Liu, Y. (2020). Three dimensional core-shell structured liquid metal/elastomer composite via coaxial direct ink writing for electromagnetic interference shielding. *Composites Part A: Applied Science and Manufacturing, 136*, Article 105957.

Wu, C., Li, Y., Sun, L., Lu, Y., Tong, C., Wang, L., Yan, Z., & Pang, J. (2020). Novel konjac glucomannan films with oxidized chitin nanocrystals immobilized red cabbage anthocyanins for intelligent food packaging. *Food Hydrocolloids, 98*, Article 105245.

Xu, F., Liu, S., Liu, Y., Xu, J., Liu, T., & Dong, S. (2019). Effectiveness of lysozyme coatings and 1-MCP treatments on storage and preservation of kiwifruit. *Food Chemistry, 288*, 201-207.

Yang, L., Liu, J., Wang, X., Wang, R., Ren, F., Zhang, Q., Shan, Y., & Ding, S. (2019). Characterization of volatile component changes in jujube fruits during cold storage by using headspace-gas chromatography-ion mobility spectrometry. *Molecules, 24*(21), Article 3904.

Yong, H., Wang, X., Zhang, X., Liu, Y., Qin, Y., & Liu, J. (2019). Effects of anthocyanin-rich purple and black eggplant extracts on the physical, antioxidant and pH-sensitive properties of chitosan film. *Food Hydrocolloids, 94*, 93-104.

Zhu, X., Song, Z., Li, Q., Li, J., Chen, W., & Li, X. (2020). Physiological and transcriptomic analysis reveals the roles of 1-MCP in the ripening and fruit aroma quality of banana fruit (Fenjiao). *Food Res Int, 130,* Article 108968.

Credit Author Statement

Zhou Wei: Conceptualization, Methodology, Investigation, Formal analysis, Writing - Original Draft

Wu zhengguo: Conceptualization, Data Curation, Writing - Original Draft, Funding acquisition

Xie Fengwei: Writing - Review & Editing, Supervision

Tang Shuwei: Formal analysis, Validation

Fang Jiawei: Software, Validation

Wang Xiaoying: Writing - Review & Editing, Funding acquisition, Supervision, Project administration

Graphical abstract

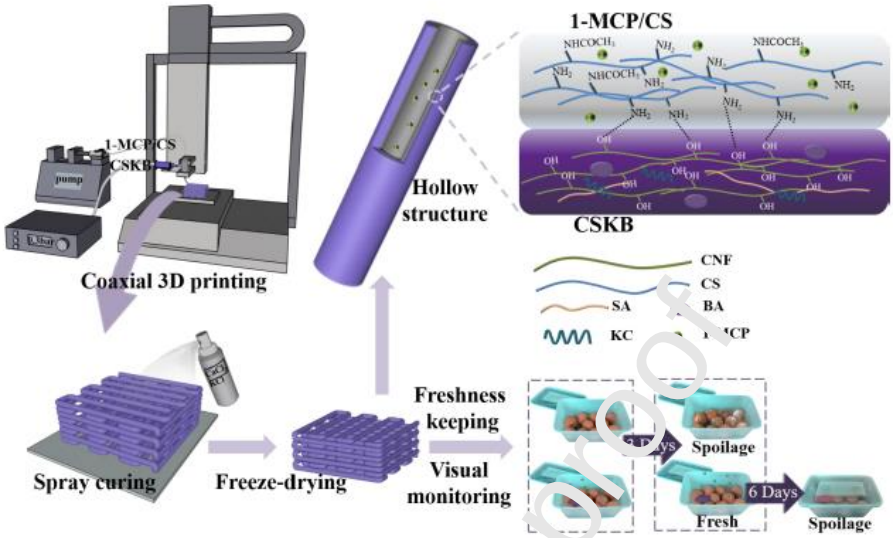

Highlights

- Nanocellulose-based fruit preservation and visual monitoring label was prepared.
- Coaxial 3D printing was applied in intelligent food packaging for the first time.
- The controlled release of 1-methylcyclopropene was realized by coaxial 3D printing.
- The shelf life of litchis was extended by 6 days.
- Chromatography-ion mobility spectrometry verified the accuracy of label indication.